

Pushing Single-Oxygen-Atom-Bridged Bimetallic Systems to the Right: A Cryptand-Encapsulated Co–O–Co Unit

Julia M. Stauber,[†] Eric D. Bloch,^{‡,†} Konstantinos D. Vogiatzis,^{||} Shao-Liang Zheng,[‡] Ryan G. Hadt,[§] Dugan Hayes,[§] Lin X. Chen,[§] Laura Gagliardi,^{*,||} Daniel G. Nocera,^{*,‡} and Christopher C. Cummins^{*,†}

[†]Department of Chemistry, Massachusetts Institute of Technology, Cambridge, Massachusetts 02139, United States

[‡]Department of Chemistry and Chemical Biology, Harvard University, Cambridge, Massachusetts 02138, United States

^{||}Department of Chemistry, Chemical Theory Center, and Supercomputing Institute, University of Minnesota, Minneapolis, Minnesota 55455, United States

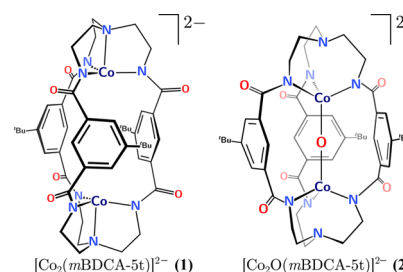
[§]Chemical Sciences and Engineering Division, Argonne National Laboratory, Lemont, Illinois 60439, United States

Supporting Information

ABSTRACT: A dicobalt(II) complex, $[\text{Co}_2(\text{mBDCA-5t})]^{2-}$ (**1**), demonstrates a cofacial arrangement of trigonal monopyramidal Co(II) ions with an inter-metal separation of 6.2710(6) Å. Reaction of **1** with potassium superoxide generates an encapsulated Co–O–Co core in the dianionic complex, $[\text{Co}_2\text{O}(\text{mBDCA-5t})]^{2-}$ (**2**); to form the linear Co–O–Co core, the inter-metal distance has diminished to 3.994(3) Å. Co K-edge X-ray absorption spectroscopy data are consistent with a +2 oxidation state assignment for Co in both **1** and **2**. Multireference complete active space calculations followed by second-order perturbation theory support this assignment, with hole equivalents residing on the bridging O-atom and on the cryptand ligand for the case of **2**. Complex **2** acts as a 2- e^- oxidant toward substrates including CO and H₂, in both cases efficiently regenerating **1** in what represent net oxygen-atom-transfer reactions. This dicobalt system also functions as a catalase upon treatment with H₂O₂.

Single-oxygen-atom-bridged bimetallic (M–O–M) systems are encountered as stable resting states or as proposed reactive intermediates in chemistry¹ and biology,² but only for the early transition metals. Hundreds of Fe–O–Fe systems exist when Fe resides in a +3 formal oxidation state, where the total d electron count is 10.³ Only three compounds have been reported for a mixed-valence Fe²⁺–O–Fe³⁺ complex, and one Fe²⁺–O–Fe²⁺ complex is known.⁴ The absence of well-characterized M–O–M systems for metals in the +2 formal oxidation state, and more generally, for total d electron counts >10, is a direct consequence of the electronic considerations embodied by the “oxo wall”.⁵ For metals right of the oxo wall, the M–O–M framework has been structurally characterized only for a Co⁶ and a Ni complex,⁷ and when the single O on Co is complexed by a Lewis acid.⁸ The zeolite catalysts Cu-ZSM-5 and Cu-MOR have been characterized as having $[\text{Cu}_2\text{O}]^{2+}$ active sites that are formed upon either O₂ or N₂O activation and are responsible for the selective oxidation of methane to methanol.⁹ Considering the rare nature of well-characterized M–O–M molecular systems for later transition metals, combined with the potential for high/novel reactivity, led us to target the stabilization of such a

Chart 1. Dicobalt Complex $[\text{Co}_2(\text{mBDCA-5t})]^{2-}$ and Oxygen-Bridged Dicobalt Complex $[\text{Co}_2\text{O}(\text{mBDCA-5t})]^{2-}$



structural unit by utilizing a robust macrobicyclic hexacarboxamide cryptand architecture for M–O–M encapsulation.

The cryptand used in the present investigation, *m*BDCA-5t-H₆ (Chart 1), and related variants, have been investigated previously for their anion receptor properties. For example, Bowman-James et al. showed that such hexacarboxamide cryptands are able to bind fluoride ion with high affinity,¹⁰ and we demonstrated the encapsulation-driven disproportionation of superoxide.¹¹ We also showed that such cryptands can function as binucleating ligands for 3d transition metal cations upon hexa-deprotonation; specifically the dimetal(II) derivatives of the cryptand have been prepared and characterized for M = Mn, Fe, Co, Ni, and Zn.¹² Cofacial bimetallic systems have a rich history for multielectron redox reactions of small molecules, particularly in the context of linked porphyrin systems.¹³ In contrast, the present hexacarboxamide cryptand system offers the opportunity to probe the combination of a cofacial bimetallic arrangement with trigonal rather than tetragonal metal ion coordination.

Double insertion of Co(II) into the cryptand proceeds upon hexa-deprotonation of *m*BDCA-5t-H₆ with $\text{K}[\text{N}(\text{SiMe}_3)_2]$ in the presence of $\text{Co}(\text{OAc})_2$ to afford the $[\text{K}_2(\text{DMF})_3]^{2+}$ salt of **1** (Chart 1) as a turquoise powder in 86% yield. Details of the synthesis and characterization of **1** by ESI-MS (negative mode), ¹H NMR, EAS, and IR are given in the Supporting Information (SI) (Figures S1–S5). Crystals suitable for X-ray diffraction study (XRD) were obtained by vapor diffusion of diethyl ether into a

Received: September 18, 2015

Published: November 11, 2015

DMF solution of the salt; Figure S13 shows a thermal ellipsoid plot of **1**. The Co...Co distance in **1**, 6.2710(6) Å, is slightly shorter than we reported previously (avg 6.4078 Å) for the analogous di-Co(II) derivative, $[\text{Co}_2(\text{mBDCA-Sp})]^{2-}$,¹² which differs in having -O-3,5-C₆H₃(O^tPr)₂ substituents in place of *t*-Bu groups on each of the three aromatic spacer components.

A useful spectroscopic signature for **1** is the broad ($\Delta\nu_{1/2}$ 76 Hz) and paramagnetically shifted (δ 6.64 ppm, DMSO-*d*₆) ¹H NMR signal (Figure S1) assigned to the three ^tBu groups that are the substituents on the three aromatic spacer components connecting the two tren metal-binding pockets of the cryptand.

Exposure of solutions of **1** to an excess of O₂ did not lead to an obvious color change, nor did it affect the ¹H NMR spectrum of **1** (Figure S30). However, monitoring the **1**/O₂ system by UV/vis spectroscopy over 90 min revealed a general increase in intensity of the bands in the visible region of the spectrum that maximized near 420 nm and was reversed upon sparging with Ar (Figure S31). Essentially identical behavior was reported recently for the closely related mononuclear TMP Co(II) complexes $[\text{Co}(\text{TEt})]^-$ and $[\text{Co}(\text{TNBn})]^-$;¹⁵ these complexes of a tren-derived tris-carboxamide ligand may be regarded as modeling one-half of **1**. Since Co(III) superoxo complexes are expected to have intense UV/vis charge-transfer bands with molar absorptivities on the order of $\epsilon = 10^4 \text{ M}^{-1} \text{ cm}^{-1}$, the minor intensity increase observed for features in the electronic spectrum of **1** upon treatment with O₂ indicates that formation of a putative **1**·O₂ adduct occurs only to a minor extent, at most.

Electrochemically, **1** displays an irreversible oxidation (Figure S65), as has been observed for closely related mononuclear TMP complexes,¹⁵ leading to the conclusion that Co(III) with low coordination number is unstable. Exceptions to this contention are Power's neutral three-coordinate hexamethyldisilazide complex $\text{Co}(\text{N}[\text{SiMe}_3]_2)_3$ ¹⁶ and Borovik's mononuclear, trigonal, open-shell Co(III) derivatives (TBP geometry) prepared using tren-based ligands.^{8b} These complexes are obtained from the oxidation of their corresponding Co(II) analogues. Accordingly, treatment of **1** with an excess of potassium superoxide, together with solubilizing 18-crown-6, led to a color change from blue (λ_{max} 596 nm, Figure S3) to dark purple (λ_{max} 581 nm, Figure S8) upon thorough mixing. Ultimately from this reaction mixture the oxidized product, dianion $[\text{Co}_2\text{O}(\text{mBDCA-Sp})]^{2-}$ (**2**), could be isolated in pure form (84% yield) as its $[\text{K}(18\text{-crown-6})]^+$ salt, a purple solid. A key spectroscopic signature of the new molecular "cobaltic oxide" dianion is the ¹H NMR signal for the three cryptand *t*-Bu substituents: δ -0.36 ppm (DMSO-*d*₆, 20 °C, Figure S6). This signature for **2** was unaffected upon replacing 18-crown-6 with Kryptofix-222 as the potassium ion complexant, and it is noticeably sharper ($\Delta\nu_{1/2}$ 21 Hz) than the corresponding signal for **1**. We note that treatment of solutions of **1** with common oxygen-atom-transfer (OAT) reagents, such as pyridine-*N*-oxide, MesCNO,¹⁷ PhIO, and Me₃NO, led to no observed reaction.

The use of a salt of superoxide¹⁸ in the synthesis of **2** deserves comment. While not a typical OAT reagent, electrochemically generated superoxide has been employed for epoxidation using metal porphyrin catalysts in conjunction with an electrophile.¹⁹ Also relevant is the report by Nam et al.²⁰ of a Cr(III) superoxide complex that effects OAT to phosphines and sulfides to mimic the function of the iron enzyme cysteine dioxygenase. Though synthetically convenient to use, potassium superoxide is not absolutely required for the formation of **2**, as we found that the latter could be generated as well under conditions of electrochemical O₂ reduction to superoxide (Figure S67).

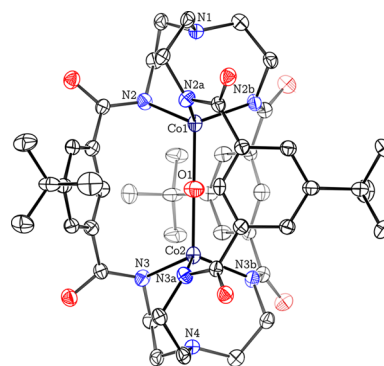


Figure 1. Solid-state structure of $[\text{Co}_2\text{O}(\text{mBDCA-Sp})]^{2-}$ (**2**) with thermal ellipsoids (drawn using PLATON¹⁴) shown at the 50% probability level. $[\text{K}(\text{Kryptofix-2,2,2})]^+$ cations, Et₂O molecules, and H-atoms omitted for clarity. A 6.2(3)% occupancy of the bimetallic cryptand site with **1** in place of **2** is likewise omitted from the drawing.²¹ Selected interatomic distances (Å) and angles (deg): Co1–N1 2.780(5), Co1–N2 2.053(6), Co2–N3 2.052(6), Co2–N4 2.786(7), Co1–O1 2.000(11), Co2–O1 1.995(11), Co1–Co2 3.994(3), O1–Co1–N2 109.29(18), N2–Co1–N2a 109.65(18), O1–Co2–N3 109.23(18), N3–Co2–N3a 109.71(18), Co1–O1–Co2 180.0(0).

Crystals of **2** as the $[\text{K}(\text{Kryptofix-222})]^+$ salt were grown by vapor diffusion of diethyl ether into a saturated DMF solution. Single-crystal XRD provided the structure displayed in Figure 1.²¹ Dianion **2** in this structure has nearly idealized C_{3h} point group symmetry, and the linear Co–O–Co core resides on a crystallographic three-fold axis of rotation. The Co sites in the structure of **2** (Figure 1) experience a nearly ideal tetrahedral N₃O coordination environment, with the metal ions pulled more toward the center of the cryptand inner space, out of bonding distance with respect to the axial amine donors and with a metal–metal distance more than 2 Å shorter vis-à-vis **1**. Accordingly, the τ_4 value of 1.00 for the Co centers in **2** reflects the near-perfect tetrahedral geometry, as compared to the value of 0.85 for **1**.²²

Upon formation of the oxo core, we would formally expect the Co oxidation state to be best described as Co³⁺–O²⁻–Co³⁺. However, because examples of tetrahedral Co(III) are extremely rare,²³ together with the novelty of a Co–O–Co core, bond valence sum (BVS) analysis²⁴ was performed in order to develop insight into the Co oxidation state. The Co–N and Co–O distances provided in the caption to Figure 1 lead to BVS-derived²⁴ oxidation states of 1.90 for both Co1 and Co2 in the structure of **2** (as compared to 2.27 for **1**). This is both interesting and surprising, suggesting that Co does not undergo oxidation upon effective O-atom addition to **1** in the course of forming $[\text{Co}_2\text{O}(\text{mBDCA-Sp})]^{2-}$ (**2**) but remains Co(II).

To assess the electronic nature of the Co–O–Co core more thoroughly, **2** was examined computationally using the complete active space (CASSCF) method followed by second-order perturbation theory (CASPT2). The CASPT2 method was chosen because the wave function that describes the antiferromagnetically coupled Co centers has a strong multireference character, with several competing configurations. Computational details of the CASSCF/CASPT2 calculations and comparison with broken-symmetry density functional theory are included in the SI (section S22). The ground state of **2** is a low-spin singlet (Figure S72), with two antiferromagnetically coupled Co centers of $S = 3/2$, one electron hole located on the bridging O-atom, analogous to a recently reported Rh–N–Rh complex,²⁵ and another electron hole located on the carboxamide of the cryptand ligand. The bridging O-atom has oxyl character ($S = 1/2$) and is

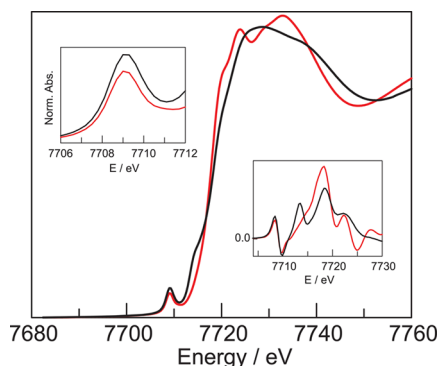
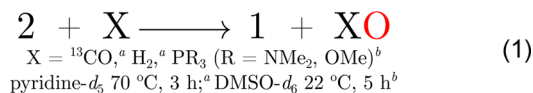


Figure 2. Co K-edge XAS data for **1** (black lines) and **2** (red lines). Top left inset, expansion of the low-energy, low-intensity $1s \rightarrow 3d$ pre-edge transition; bottom right inset, first derivative of the edge region.

through-space antiferromagnetically coupled to the cryptand ligand ($S = 1/2$). Coupling of the four spin centers gives rise to a spin ladder composed of two singlets, four triplets, four quintets, three septets, and one nonet spin states. All states of the spin ladder are within an energy range of $\sim 1730 \text{ cm}^{-1}$, while the first excited state was higher by $>22\,000 \text{ cm}^{-1}$, which is assigned to a d-d band. Therefore, the multireference calculation indicates that the $2-e^-$ oxidation of **1** to **2** is not metal centered but is ligand centered with an oxygen- and cryptand-based parentage.

X-ray absorption near-edge spectroscopy of **1** and **2** confirms that the metal centers remain as Co(II) upon the oxidation of **1** to **2** (Figure 2). Both the Co K pre-edge and edge energy positions are indicators of Co oxidation state. The observed pre-edge ($\sim 7709 \text{ eV}$) and edge energy positions ($\sim 7718 \text{ eV}$; right inset in Figure 2) do not change on going from **1** to **2**, consistent with a lack of significant oxidation state change.²⁶ The former is in exact agreement with the value (7709 eV) displayed by a reference compound, Co_3O_4 , containing tetrahedral Co(II) centers. This interpretation is in good agreement with magnetism data for **2** (SQUID magnetometry, Figure S64), which suggest an integer-spin system consistent with the observation that **2** is EPR-silent. The absence of EPR signals for bimetallic Co(II) centers is indicative of weak antiferromagnetic coupling. Indeed, weakly coupled ($J = -1.6$ as compared to -0.5 for **1**) bimetallic Co(II) systems have been shown to be EPR silent.²⁷

We probed the capacity of **2** as an oxidant (eq 1) beginning with PR_3 ($R = \text{NMe}_2, \text{OMe}$) substrates. Both of these substrates

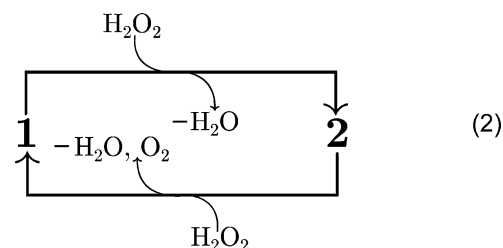


were found to effect the reduction of **2** to **1**, as assayed using the ^1H NMR signatures ($t\text{Bu}$ signal, Figures S53, S56), while ^{31}P monitoring revealed the concomitant formation of the corresponding OPR_3 compound (Figures S52, S55). Triphenylphosphine, which forms a weaker phosphoryl $\text{P}=\text{O}$ bond than the latter two successful substrates,²⁸ was not seen to be oxidized by **2** under the same conditions, nor was it found to regenerate **1**.

Carbon monoxide is a modestly weaker deoxygenating agent than triphenylphosphine from the standpoint of bond dissociation enthalpies (127.2 vs 132.2 kcal/mol , respectively),^{17,29} but we find CO to be competent for the reduction of **2** back to **1**. Confirmation of $^{13}\text{CO}_2$ as the product of oxidation was facilitated by carrying out this experiment using ^{13}CO and monitoring the ^{13}C NMR spectrum (Figure S43).

At 117.4 kcal/mol (bond dissociation enthalpy for $\text{H}_2\text{O} \rightarrow \text{H}_2 + \text{O}$, using standard gas-phase heats of formation for H_2O and for the O-atom), molecular hydrogen is a still less potent O-atom acceptor than carbon monoxide, yet it reacts with **2** similarly to regenerate **1** (eq 1, Figures S48–S50). Since the reaction with H_2 should produce 1 equiv of water, we also tested the stability of **1** and **2** in the presence of excess water. For these experiments, water (as much as ~ 650 equiv) was added to DMSO- d_6 solutions of potassium salts of **1** and **2**. No color change was observed upon mixing at 20°C , and subsequent analysis by ^1H NMR spectroscopy showed that both **1** and **2** were persistent under these conditions in the presence of water and had not undergone degradation (Figures S18–S23).

Given the stability of **1** and **2** to water (and O_2), we decided to probe for possible catalase activity stemming from the present cobalt/cryptand system. While many manganese complexes exhibit catalase activity,³⁰ catalase model systems based upon Co are rare.³¹ Moreover, in these reactions the metal oxo is typically the resting state. In the present cobalt/cryptand system, the unusual situation exists where disproportionation may be promoted from the isolable reduced compound **1** and metal oxo compound **2**. In a typical run, to a DMF solution of $[\text{K}_2(\text{DMF})_3][\mathbf{1}]$ was added aqueous hydrogen peroxide from a stock solution prepared by dissolving urea hydrogen peroxide (UHP, ~ 400 equiv) in water, and the ensuing reaction which took place with vigorous gas evolution was then monitored using a pressure transducer (Figures S32, S33). The catalase reaction proceeded until H_2O_2 consumption was essentially complete, and the identity of the evolved gas as O_2 was confirmed by GC (Figure S27). NMR experiments further showed that **1** is effectively unchanged after treatment with a stoichiometric amount of aqueous UHP (Figure S28); given the same treatment, **2** is converted back into **1** (Figure S29). The overall cycle is as shown in eq 2. Both **1** and **2** are reactive toward H_2O_2 , and both



appear competent to be involved in the catalytic cycle; the present system constitutes a rare example of a functional catalase model that is isolable and structurally well defined in both the oxidized and reduced states.

The cryptand complex of $\text{Co}-\text{O}-\text{Co}$ “pushes MOM to the right” with the stabilization of an oxo having a total d electron count >10 . By preparing a molecular oxidant that is based upon a linear $\text{M}-\text{O}-\text{M}$ core using a 3d metal to the right of iron in the periodic table, we herein identify a structure–activity relationship for a species that is rendered isolable through the use of a robust, hexacarboxamide cryptand ligand architecture. Moving forward, interesting questions to be addressed revolve around both the scope of metal ions amenable to such a modality and the range of substrates susceptible to oxidation by new $\text{M}-\text{O}-\text{M}$ complexes.

■ ASSOCIATED CONTENT

📄 Supporting Information

The Supporting Information is available free of charge on the ACS Publications website at DOI: 10.1021/jacs.5b09827.

X-ray data for $[K_2(DMF)_3][1]$ (CIF)
X-ray data for $[K(Kryptofix-2,2,2)]_2[2]$ (CIF)
Experimental procedures and characterization data (PDF)

AUTHOR INFORMATION

Corresponding Authors

*gagliard@umn.edu
*dnocera@fas.harvard.edu
*cummins@mit.edu

Notes

The authors declare no competing financial interest.

ACKNOWLEDGMENTS

This Communication is based upon work supported by the National Science Foundation under CHE1305124 and by the U.S. Department of Energy (DOE) under DE-SC0009565. R.G.H. is supported by the Laboratory Directed Research and Development (LDRD) program at Argonne National Laboratory. D.H. is supported by the Joseph J. Katz Postdoctoral Fellowship at Argonne National Laboratory (ANL). Work at ANL was supported by funding from the Division of Chemical Sciences, Biosciences, Office of Basic Energy Sciences, DOE, through Grant DE-AC02-06CH11357. Use of Beamline 12BM at the Advanced Photon Source was supported by the DOE under Contract No. DE-AC02-06CH11357. The computational part of this work was supported in part by the DOE, Office of Basic Energy Sciences, under SciDAC grant no. DE-SC0008666 (K.V. and L.G.). We acknowledge the Minnesota Supercomputing Institute (MSI) at the University of Minnesota for providing the computational resources, Sungsik Lee for help in making XAS measurements, Nazario Lopez and Glen Alliger for contributions developing cobalt/cryptand synthetic methods, and Varinia Bernaldes for fruitful discussions on the DFT calculations.

REFERENCES

- (1) (a) Barats-Damatov, D.; Shimon, L. J. W.; Weiner, L.; Schreiber, R. E.; Jimenez-Lozano, P.; Poblet, J. M.; de Graff, C.; Neumann, R. *Inorg. Chem.* **2014**, *53*, 1779. (b) Shan, J.; Huang, W.; Nguyen, L.; Yu, Y.; Zhang, S.; Li, Y.; Frenkel, A. I.; Tao, F. *Langmuir* **2014**, *30*, 8558.
- (2) Que, L., Jr.; True, A. E. *Prog. Inorg. Chem.* **1990**, *38*, 97.
- (3) (a) Hoffman, A. B.; Collins, D. M.; Day, V. W.; Fleischer, E. B.; Srivastava, T. S.; Hoard, J. L. *J. Am. Chem. Soc.* **1972**, *94*, 3620. (b) Murray, K. S. *Coord. Chem. Rev.* **1974**, *12*, 1. (c) Norman, R. E.; Holz, R. C.; Menage, S.; Que, L., Jr.; Zhang, J. H.; O'Connor, C. J. *Inorg. Chem.* **1990**, *29*, 4629. (d) Kodera, M.; Shimakoshi, H.; Nishimura, M.; Okawa, H.; Iijima, S.; Kano, K. *Inorg. Chem.* **1996**, *35*, 4967. (e) Tshuva, E. Y.; Lippard, S. J. *Chem. Rev.* **2004**, *104*, 987.
- (4) (a) Arena, F.; Floriani, C.; Chiesi-Villa, A.; Guastini, C. J. *Chem. Soc., Chem. Commun.* **1986**, 1369. (b) Payne, S. C.; Hagen, K. S. *J. Am. Chem. Soc.* **2000**, *122*, 6399. (c) Eckert, N. A.; Stoian, S.; Smith, J. M.; Bominaar, E. L.; Münck, E.; Holland, P. L. *J. Am. Chem. Soc.* **2005**, *127*, 9344.
- (5) Winkler, J. R.; Gray, H. B. In *Structure and Bonding*; Mingos, D. M. P., Day, P., Dahl, J. P., Eds.; Springer: Berlin, 2012; Vol. 142, pp 17–28.
- (6) Zhang, R.-L.; Zhao, J.-S.; Xi, X.-L.; Yang, P.; Shi, Q.-Z. *Chin. J. Chem.* **2008**, *26*, 1225.
- (7) Bag, B.; Mondal, N.; Rosair, G.; Mitra, S. *Chem. Commun.* **2000**, 1729.
- (8) (a) Pfaff, F. F.; Kundu, S.; Risch, M.; Pandian, S.; Heims, F.; Pryjomska-Ray, I.; Haack, P.; Metzinger, R.; Bill, E.; Dau, H.; Comba, P.; Ray, K. *Angew. Chem., Int. Ed.* **2011**, *50*, 1711. (b) Lacy, D. C.; Park, Y. J.; Ziller, J. W.; Yano, J.; Borovik, A. S. *J. Am. Chem. Soc.* **2012**, *134*, 17526. (c) Hong, S.; Pfaff, F. F.; Kwon, E.; Wang, Y.; Seo, M.-S.; Bill, E.; Ray, K.; Nam, W. *Angew. Chem., Int. Ed.* **2014**, *53*, 10403.
- (9) (a) Vanelderen, P.; Snyder, B. E. R.; Tsai, M.-L.; Hadt, R. G.; Vancauwenbergh, J.; Coussens, O.; Schoonheydt, R. A.; Sels, B. F.;

Solomon, E. I. *J. Am. Chem. Soc.* **2015**, *137*, 6383. (b) Tsai, M.-L.; Hadt, R. G.; Vanelderen, P.; Sels, B. F.; Schoonheydt, R. A.; Solomon, E. I. *J. Am. Chem. Soc.* **2014**, *136*, 3522. (c) Smeets, P. J.; Hadt, R. G.; Woertink, J. S.; Vanelderen, P.; Schoonheydt, R. A.; Sels, B. F.; Solomon, E. I. *J. Am. Chem. Soc.* **2010**, *132*, 14736.

(10) (a) Kang, S. O.; Llinares, J. M.; Powell, D.; VanderVelde, D.; Bowman-James, K. *J. Am. Chem. Soc.* **2003**, *125*, 10152. (b) Kang, S. O.; Llinares, J. M.; Day, V. W.; Bowman-James, K. *Chem. Soc. Rev.* **2010**, *39*, 3980. (c) Kang, S. O.; Day, V. W.; Bowman-James, K. *J. Org. Chem.* **2010**, *75*, 277.

(11) Lopez, N.; Graham, D. J.; McGuire, R., Jr.; Alliger, G. E.; Shao-Horn, Y.; Cummins, C. C.; Nocera, D. G. *Science* **2012**, *335*, 450.

(12) (a) Alliger, G. E.; Mueller, P.; Cummins, C. C.; Nocera, D. G. *Inorg. Chem.* **2010**, *49*, 3697. (b) Alliger, G. E.; Mueller, P.; Do, L. H.; Cummins, C. C.; Nocera, D. G. *Inorg. Chem.* **2011**, *50*, 4107.

(13) (a) Collman, J. P.; Wagenknecht, P. S.; Hutchison, J. E. *Angew. Chem., Int. Ed. Engl.* **1994**, *33*, 1537. (b) Deng, Y.; Chang, C. J.; Nocera, D. G. *J. Am. Chem. Soc.* **2000**, *122*, 410.

(14) (a) Spek, A. L. *J. Appl. Crystallogr.* **2003**, *36*, 7. (b) Spek, A. L. *Acta Crystallogr.* **2009**, *D65*, 148.

(15) (a) Blacquiere, J. M.; Pegis, M. L.; Raugei, S.; Kaminsky, W.; Forget, A.; Cook, S. A.; Taguchi, T.; Mayer, J. M. *Inorg. Chem.* **2014**, *53*, 9242. (b) Dai, X.; Kapoor, P.; Warren, T. H. *J. Am. Chem. Soc.* **2004**, *126*, 4798. (c) Jones, C.; Schulten, C.; Rose, R. P.; Stasch, A.; Aldridge, S.; Woodul, W. D.; Murray, K. S.; Moubaraki, B.; Brynda, M.; La Macchia, G.; Gagliardi, L. *Angew. Chem., Int. Ed.* **2009**, *48*, 7406.

(16) Ellison, J. J.; Power, P. P.; Shoner, S. C. *J. Am. Chem. Soc.* **1989**, *111*, 8044.

(17) (a) Cai, X.; Majumdar, S.; Fortman, G. C.; Frutos, L. M.; Temprado, M.; Clough, C. R.; Cummins, C. C.; Germain, M. E.; Palluccio, T.; Rybak-Akimova, E. V.; Captain, B.; Hoff, C. D. *Inorg. Chem.* **2011**, *50*, 9620. (b) Palluccio, T. D.; Rybak-Akimova, E. V.; Majumdar, S.; Cai, X.; Chui, M.; Temprado, M.; Silvia, J. S.; Cozzolino, A. F.; Tofan, D.; Velian, A.; Cummins, C. C.; Captain, B.; Hoff, C. D. *J. Am. Chem. Soc.* **2013**, *135*, 11357.

(18) Sawyer, D. T.; Valentine, J. S. *Acc. Chem. Res.* **1981**, *14*, 393.

(19) Ojima, F.; Kobayashi, N.; Osa, T. *Bull. Chem. Soc. Jpn.* **1990**, *63*, 1374.

(20) Cho, J.; Woo, J.; Nam, W. *J. Am. Chem. Soc.* **2012**, *134*, 11112.

(21) The observed ratio of 2:1 in solution from a ^1H NMR spectrum of a sample of the same batch of crystals was 93:7 in DMSO- d_6 .

(22) Yang, L.; Powell, D. R.; Houser, R. P. *J. Chem. Soc., Dalton Trans.* **2007**, 955.

(23) Kozhukh, J.; Minier, M. A.; Lippard, S. J. *Inorg. Chem.* **2015**, *54*, 418.

(24) (a) Palenik, G. J. *Inorg. Chem.* **1997**, *36*, 122. (b) Mahapatra, S.; Halfen, J. A.; Wilkinson, E. C.; Pan, G.; Wang, X.; Young, V. G., Jr.; Cramer, C. J.; Que, L., Jr.; Tolman, W. B. *J. Am. Chem. Soc.* **1996**, *118*, 11555.

(25) Gloaguen, Y.; Rebreyend, C.; Lutz, M.; Kumar, P.; Huber, M.; van der Vlugt, J. I.; Schneider, S.; de Bruin, B. *Angew. Chem., Int. Ed.* **2014**, *53*, 6814.

(26) (a) Poltavets, V. V.; Croft, M.; Greenblatt, M. *Phys. Rev. B* **2006**, *74*, 125103. (b) Kanan, M. W.; Yano, J.; Surendranath, Y.; Dincă, M.; Yachandra, V. K.; Nocera, D. G. *J. Am. Chem. Soc.* **2010**, *132*, 13692.

(27) Schultz, B. E.; Ye, B.-H.; Li, X.-Y.; Chan, S. I. *Inorg. Chem.* **1997**, *36*, 2617.

(28) Holm, R. H.; Donahue, J. P. *Polyhedron* **1993**, *12*, 571.

(29) Luo, Y.-R. *Handbook of bond dissociation energies in organic compounds*; CRC Press: Boca Raton, 2003.

(30) Wu, A. J.; Penner-Hahn, J. E.; Pecoraro, V. L. *Chem. Rev.* **2004**, *104*, 903.

(31) Yamami, M.; Tanaka, M.; Sakiyama, H.; Koga, T.; Kobayashi, K.; Miyasaka, H.; Ohba, M.; Okawa, H. *J. Chem. Soc., Dalton Trans.* **1997**, 4595.